Right atrial adaptation to precapillary pulmonary hypertension: pressure-volume, cardiomyocyte, and histological analysis

Wessels, J.N.; Wezenbeek, J. van; Rover, J. de; Smal, R.; Llucià-Valldeperas, A.; Celant, L.R.; ... ; Man, F.S. de

JOURNAL OF THE AMERICAN COLLEGE OF CARDIOLOGY VOL. 82, NO. 8, 2023

Right Atrial Adaptation to Precapillary Pulmonary Hypertension

Pressure-Volume, Cardiomyocyte, and Histological Analysis

Jeroen N. Wessels, MD,[a,b,*] Jessie van Wezenbeek, MSc,[a,b,*] Jari de Rover, BSc,[c] Rowan Smal, MSc,[a,b] Aida Llucià-Valldeperas, PhD,[a,b] Lucas R. Celant, MD,[a,b] J. Tim Marcus, PhD,[b,d] Lilian J. Meijboom, MD, PhD,[b,d] Joanne A. Groeneveldt, MD,[a,b] Frank P.T. Oosterveer, BSc,[a,b] Toon A. Winkelman, MD,[e] Hans W.M. Niessen, MD, PhD,[f] Marie-José Goumans, PhD,[g] Harm Jan Bogaard, MD, PhD,[a,b] Anton Vonk Noordegraaf, MD, PhD,[a,b] Gustav J. Strijkers, PhD,[h] M. Louis Handoko, MD, PhD,[b,i] Berend E. Westerhof, PhD,[a,b] Frances S. de Man, PhD[a,b]

ABSTRACT

BACKGROUND Precapillary pulmonary hypertension (precPH) patients have altered right atrial (RA) function and right ventricular (RV) diastolic stiffness.

OBJECTIVES This study aimed to investigate RA function using pressure-volume (PV) loops, isolated cardiomyocyte, and histological analyses.

METHODS RA PV loops were constructed in control subjects (n = 9) and precPH patients (n = 27) using magnetic resonance and catheterization data. RA stiffness (pressure rise during atrial filling) and right atrioventricular coupling index (RA minimal volume / RV end-diastolic volume) were compared in a larger cohort of patients with moderate (n = 39) or severe (n = 41) RV diastolic stiffness. Cardiomyocytes were isolated from RA tissue collected from control subjects (n = 6) and precPH patients (n = 9) undergoing surgery. Autopsy material was collected from control subjects (n = 6) and precPH patients (n = 4) to study RA hypertrophy, capillarization, and fibrosis.

RESULTS RA PV loops showed 3 RA cardiac phases (reservoir, passive emptying, and contraction) with dilatation and elevated pressure in precPH. PrecPH patients with severe RV diastolic stiffness had increased RA stiffness and worse right atrioventricular coupling index. Cardiomyocyte cross-sectional area was increased 2- to 3-fold in precPH, but active tension generated by the sarcomeres was unaltered. There was no increase in passive tension of the cardiomyocytes, but end-stage precPH showed reduced number of capillaries per mm^2 accompanied by interstitial and perivascular fibrosis.

CONCLUSIONS RA PV loops show increased RA stiffness and suggest atrioventricular uncoupling in patients with severe RV diastolic stiffness. Isolated RA cardiomyocytes of precPH patients are hypertrophied, without intrinsic sarcomeric changes. In end-stage precPH, reduced capillary density is accompanied by interstitial and perivascular fibrosis. (J Am Coll Cardiol 2023;82:704–717) © 2023 The Authors. Published by Elsevier on behalf of the American College of Cardiology Foundation. This is an open access article under the CC BY-NC-ND license (http://creativecommons.org/licenses/by-nc-nd/4.0/).

Listen to this manuscript's audio summary by Editor-in-Chief Dr Valentin Fuster on www.jacc.org/journal/jacc.

From the [a]PHEniX Laboratory, Department of Pulmonary Medicine, Amsterdam UMC location Vrije Universiteit Amsterdam, Amsterdam, the Netherlands; [b]Pulmonary Hypertension and Thrombosis, Amsterdam Cardiovascular Sciences, Amsterdam, the Netherlands; [c]Cardiovascular and Respiratory Physiology, Faculty of Science and Technology, Technical Medical Centre, University of Twente, Enschede, the Netherlands; [d]Department of Radiology and Nuclear Medicine, Amsterdam UMC location Vrije Universiteit Amsterdam, Amsterdam, the Netherlands; [e]Department of Cardiothoracic Surgery, Amsterdam UMC location University of Amsterdam, Amsterdam, the Netherlands; [f]Department of Pathology, Amsterdam UMC location Vrije Universiteit Amsterdam, Amsterdam, the Netherlands; [g]Department of Cell and Chemical Biology, Leiden UMC, Leiden, the Netherlands; [h]Department of Biomedical Engineering and Physics, Amsterdam UMC location University of Amsterdam, Amsterdam, the Netherlands; and the [i]Department of Cardiology, Amsterdam UMC location Vrije Universiteit Amsterdam, Amsterdam, the Netherlands. *Drs Wessels and van Wezenbeek contributed equally to this work.

The authors attest they are in compliance with human studies committees and animal welfare regulations of the authors' institutions and Food and Drug Administration guidelines, including patient consent where appropriate. For more information, visit the Author Center.

Manuscript received January 18, 2023; revised manuscript received May 25, 2023, accepted May 31, 2023.

ISSN 0735-1097 https://doi.org/10.1016/j.jacc.2023.05.063

The right atrium (RA) in precapillary pulmonary hypertension (precPH) has been recognized as a key clinical parameter.[1,2] The predictive value of RA pressure and volume for pulmonary arterial hypertension (PAH) mortality is confirmed in multiple studies, and both are essential in the current risk stratification of PAH patients.[3] The RA must cope with an increased pressure load due to right ventricular (RV) diastolic stiffness and an increased volume load because of tricuspid regurgitation in PAH.[4] Previous studies have indicated that RA stroke work is enhanced in precPH but does not result in increased RV filling because of RV diastolic stiffness.[5] Higher filling pressures cause vena cava backflow during atrial contraction, further increasing RA volume overload.[5,6] This may suggest a mismatch between atrial and ventricular adaptation, or altered atrioventricular coupling.

SEE PAGE 718

In-depth analysis of RA function is challenging because of the difficult physiology of the atrial cardiac cycle, which consists of 3 phases: 1) the reservoir phase, atrial filling during ventricular contraction; 2) passive emptying, during early ventricular diastole (also called conduit); and 3) atrial contraction, at the end of ventricular diastole.[7-9] In contrast to the square or triangular shape of pressure-volume (PV) loops describing ventricular function, atrial PV loops have a distinct shape.[10-13] Currently, no data are available on RA PV loops in precPH, only in animal models.[14-16] Also, analysis of RA tissue morphology and cardiomyocyte function in precPH is lacking. Therefore, the aim of this study was to fully characterize changes in the RA in precPH at 3 different levels: 1) in vivo assessment of RA function using PV loops; 2) ex vivo assessment of RA function using single-cardiomyocyte analysis; and 3) histological assessment of changes in RA hypertrophy, fibrosis, and capillary density.

ABBREVIATIONS AND ACRONYMS

CMR = cardiac magnetic resonance

CTEPH = chronic thromboembolic pulmonary hypertension

E_{ed} = end-diastolic elastance

LA = left atrium/atrial

PAH = pulmonary arterial hypertension

precPH = precapillary pulmonary hypertension

PV = pressure-volume

RA = right atrium/atrial

RACI = right atrioventricular coupling index

RV = right ventricle/ventricular

METHODS

Additional information on the Methods is provided in the Supplemental Appendix.

STUDY SUBJECTS. Figure 1 shows the 4 patient cohorts examined in this study. RA PV loops were

FIGURE 1 Overview of the 4 Patient Cohorts Used in This Study

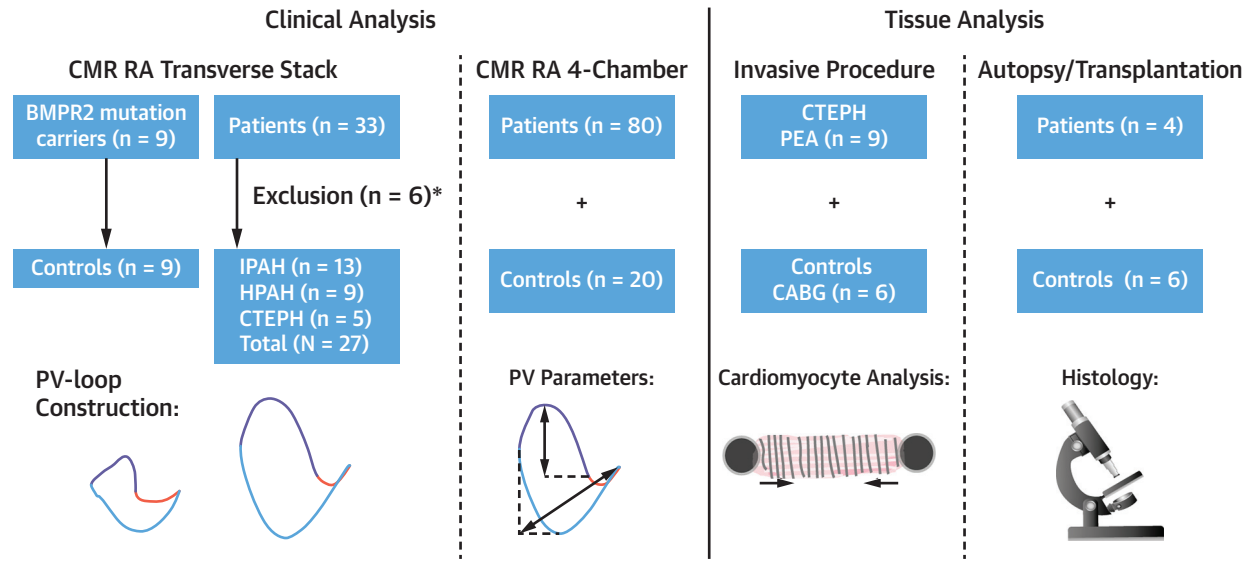

Cardiac magnetic resonance (CMR) transverse stack throughout the right atrium (RA) was available in bone morphogenic protein receptor 2 (BMPR2) mutation carriers and precapillary pulmonary hypertension patients. Pressure-volume (PV) loop parameters were estimated in a larger cohort of pulmonary arterial hypertension patients and control subjects. Cardiomyocytes were isolated from RA tissue obtained during surgery in chronic thromboembolic pulmonary hypertension (CTEPH) and coronary artery bypass grafting (CABG) patients. Histological analysis was performed in autopsy material from pulmonary arterial hypertension patients and control subjects. *A poor-quality RA pressure curve was a reason for exclusion. HPAH = hereditary pulmonary arterial hypertension; IPAH = idiopathic pulmonary arterial hypertension; PEA = pulmonary endarterectomy.

FIGURE 2 RA Volume Measurement and Example RA PV Loops

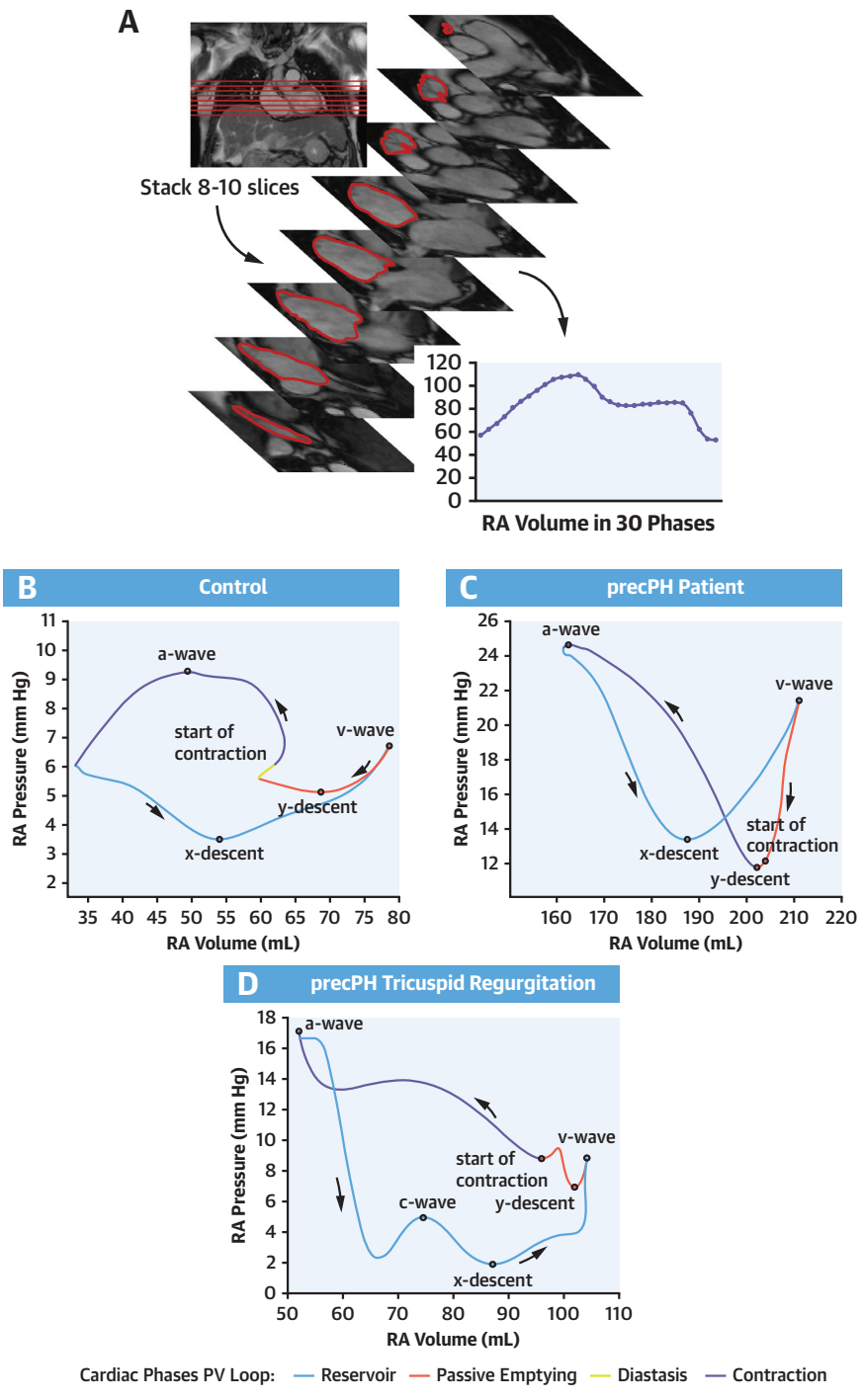

(A) Endocardial contours were drawn in a transverse stack of cine images to determine RA volume in all 30 CMR phases. The superior and inferior vena cava were carefully excluded in slices in which they were clearly separated from the atrium or when there was no wall motion during atrial contraction. Three examples of RA PV loops are given for a healthy control subject **(B)**, a precapillary pulmonary hypertension (precPH) patient **(C)**, and the only patient with significant tricuspid regurgitation **(D)**. In some control subjects, a diastasis phase can be identified during which atrial volume increases due to inflow from the vena cava. In the patient with tricuspid regurgitation, a marked c-wave can be seen (closure of the tricuspid valve). a-wave = atrial contraction at ventricular end-diastole; c-wave = a pressure increase due to tricuspid bulging into the atrium as a result of isovolumic ventricular contraction; x-descent = a drop in atrial pressure during ventricular systole caused by atrial relaxation; v-wave = atrial filling during ventricular contraction; y-descent = atrial pressure drop as blood enters the ventricle during diastole; other abbreviations as in Figure 1.

FIGURE 3 RA PV Loops in PrecPH Patients and Control Subjects

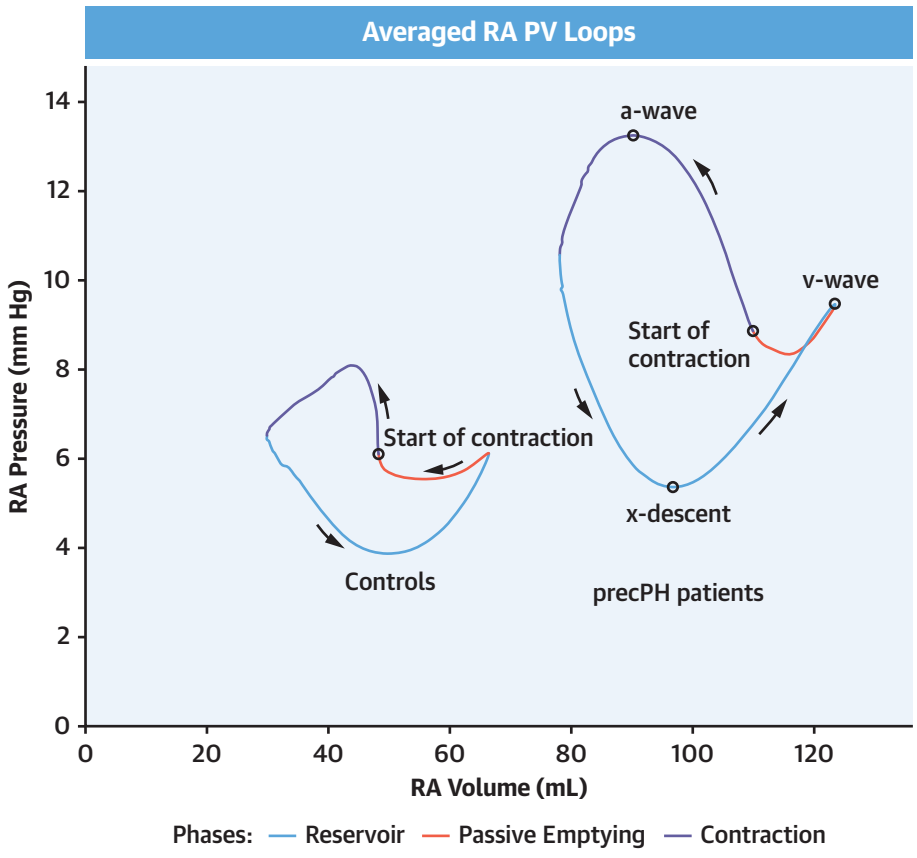

RA pressure and volume signals for the control (n = 9) and patient (n = 27) groups were averaged and subsequently plotted. The reservoir phase in **blue** depicts the filling of the atrium. Passive emptying in **red** reflects the early diastolic phase, and atrial contraction is depicted in **purple**. Abbreviations as in Figures 1 and 2.

constructed from a prospective cohort of PAH or chronic thromboembolic pulmonary hypertension (CTEPH) patients (n = 27) using RA volume determined on a cardiac magnetic resonance (CMR) transverse stack of slices. Patients were diagnosed according to European Society of Cardiology/European Respiratory Society guidelines between September 2017 and April 2021 (medical ethics review committee approval number 2017.161).[3] Healthy BMPR2 (bone morphogenic protein receptor 2) mutation carriers (n = 9) were included as control subjects (approval number 2017.318). In a larger, previously published cohort of incident PAH patients (n = 80) and control subjects (n = 20), RA PV loop parameters were derived using RA volume measured on the CMR cine 4-chamber view (approval number 2012.288).[5] Although the 4-chamber view underestimates true axial stack volumes, they correlated excellently (Pearson r correlation coefficients 0.86-0.91). RA tissue was collected from control subjects (n = 6) undergoing coronary artery bypass grafting and CTEPH patients (n = 9) undergoing pulmonary endarterectomy (approval number 2017.161). All subjects gave written informed consent for data and tissue collection. Control subjects did not show any signs of RV/RA dysfunction/dilatation or moderate/severe tricuspid regurgitation on echocardiography. During the surgical procedure, a small piece of RA tissue was obtained and put in a cardioplegic solution on ice for transportation, after which it was snap-frozen in liquid nitrogen until further analysis. In addition, for histological assessment we obtained RA tissue from deceased control subjects (n = 6) and either deceased or transplanted PAH patients (n = 4). On autopsy, no cardiac abnormalities were observed in the hearts of control subjects. For 3 of 6 control subjects and 2 of 4 PAH patients, histological analysis of RV tissue has been described before.[17]

TABLE 1 Characteristics and PV Loop Parameters in Control Subjects and Low vs High RV E_{ed} Patients

	Control (n = 20)	Low E_{ed} (n = 39)	High E_{ed} (n = 41)
Female	12 (60)	25 (64)	29 (71)
Age, y	46.6 ± 15.5	55.6 ± 17.6	57.8 ± 17.6
NYHA functional class I/II/III/IV	10/8/2/0	2/16/19/2[a]	1/11/25/4[a]
NT-proBNP, pg/mL	44 (31-95)	433 (182-1363)	1999 (901-3361)[a,b]
Reverse log-transformed, mean (95% CI)	40 (31-52)	534 (434-656)	1525 (1265-1839)
Catheterization			
mPAP, mm Hg	15.8 ± 3.6	45.7 ± 11.0[a]	55.4 ± 16.0[a,b]
PAWP, mm Hg	8.9 ± 2.4	9.4 ± 2.6	9.0 ± 3.2
Cardiac index, L/min/m^2	3.5 ± 0.9	2.7 ± 0.8[a]	2.4 ± 0.9[a]
PVR, WU	1.1 ± 0.5	7.7 ± 3.5[a]	11.5 ± 5.1[a,b]
Svo_2, %	76 ± 5	65 ± 7[a]	61 ± 11[a]
mRAP, mm Hg	5 (3-6)	5 (4-7.5)	8 (5-12)[a,b]
Reverse log-transformed, mean (95% CI)	4 (4-5)	5 (5-6)	7 (6-8)
RV function			
RV E_{ed}, mm Hg/mL	0.21 (0.14-0.25)	0.42 (0.27-0.53)[a]	0.90 (0.78-1.12)[a,b]
Reverse log-transformed, mean (95% CI)	0.17 (0.13-0.23)	0.37 (0.32-0.43)	0.95 (0.87-1.04)
RVEDVi, mL/m^2	65 ± 13	80 ± 20[a]	84 ± 22[a]
RVESVi, mL/m^2	26 ± 7	48 ± 20[a]	58 ± 20[a,b]
RVEF, %	61 ± 7	42 ± 12[a]	32 ± 10[a,b]
RV mass, g	40 ± 13	85 ± 25[a]	101 ± 34[a,b]
SVi, mL/m^2	43 ± 7	32 ± 7[a]	27 ± 9[a,b]
RA function			
RA v-wave pressure, mm Hg	5.5 (4.0-6.9)	6.4 (4.1-8.6)	8.6 (5.7-13.2)[a]
Reverse log-transformed, mean (95% CI)	5.3 (4.8-5.8)	6.2 (5.6-6.8)	7.8 (6.7-9.0)
RA p-wave pressure, mm Hg	5.4 (4.1-6.1]	5.6 (3.4-7.6]	7.1 (4.4-9.3]
RA a-wave pressure, mm Hg	8.0 (7.3-9.7]	9.1 (7.2-11.8]	13.6 (8.6-17.3][a,b]
RA x-descent pressure, mm Hg	2.0 (0.4-3.5]	2.5 (0.2-3.9]	3.5 (1.1-9.4]
RA v-wave volume, mL	82 (74-110)	129 (104-154)[a]	140 (114-180)[a]
Reverse log-transformed, mean (95% CI)	90 (78-104)	128 (118-138)	143 (125-161)
RA p-wave volume, mL	58 (50-77)	96 (85-127)[a]	119 (95-165)[a,b]
Reverse log-transformed, mean (95% CI)	64 (59-69)	104 (99-108)	119 (111-127)
RA minimum volume, mL	40 (35-48)	59 (48-80)	77 (57-119)[a,b]
Reverse log-transformed, mean (95% CI)	43 (40-47)	63 (60-67)	81 (74-88)
RA passive emptying, mL	24 (22-32)	21 (18-31)	20 (15-26)
Reverse log-transformed, mean (95% CI)	25 (21-29)	23 (20-26)	20 (17-23)
RA active emptying, mL	18 (15-28)	39 (18-60)[a]	38 (5-72)[a]
RA stiffness, mm Hg/mL	0.076 (0.060-0.098)	0.062 (0.044-0.086)	0.080 (0.059-0.127)[b]
Reverse log-transformed, mean (95% CI)	0.077 (0.065-0.090)	0.058 (0.048-0.071)	0.084 (0.070-0.100)
RASW, mm Hg·mL	175 (109-222)	350 (250-487)[a]	375 (250-746)
Reverse log-transformed, mean (95% CI)	164 (133-202)	354 (302-416)	392 (311-488)
Contractile pressure rise, mm Hg	2.8 (2.4-3.5)	3.6 (2.9-5.4)	5.4 (3.7-7.8)[a,b]
Reverse log-transformed, mean (95% CI)	2.9 (2.5-3.4)	3.7 (3.1-4.4)	5.2 (4.4-6.2)
RACI	0.36 (0.33-0.39)	0.43 (0.36-0.53)	0.52 (0.40-0.73)[a,b]
Reverse log-transformed, mean (95% CI)	0.37 (0.33-0.41)	0.43 (0.40-0.47)	0.53 (0.47-0.61)

Values are n (%), mean ± SD, n, or median (IQR), unless otherwise indicated. Non-normally distributed parameters were log-transformed prior to testing. [a]$P < 0.05$ in comparison with control group. [b]$P < 0.05$ in comparison with low E_{ed}.

E_{ed} = end-diastolic elastance; mPAP = mean pulmonary artery pressure; mRAP = mean right atrial pressure; NT-proBNP = N-terminal pro-B-type natriuretic peptide; PAWP = pulmonary arterial wedge pressure; PVR = pulmonary vascular resistance; RA = right atrial; RACI = right atrioventricular coupling index; RASW = right atrial stroke work; RV = right ventricular; RVEDVi = right ventricular end-diastolic volume index; RVEF = right ventricular ejection fraction; RVESVi = right ventricular end-systolic volume index; SVi = stroke volume index; Svo_2 = mixed venous oxygen saturation.

RIGHT HEART CATHETERIZATION. Hemodynamic assessment was performed using a balloon-tipped, flow-directed 7.5-F triple lumen Swan-Ganz catheter (Edwards Lifesciences). Pressures were recorded at rest, in sinus rhythm, during spontaneous breathing.

CARDIAC MAGNETIC RESONANCE. CMR scans were made using a Siemens 1.5-T Sonata, Avanto, or Sola scanner (Siemens Medical Solutions). Acquisition of scans and postprocessing was performed as described before.[18] A transverse stack of cine images

throughout the RA was acquired with a slice thickness of 6 mm and an interslice gap of 4 mm. Endocardial contours were drawn in applicable slices using commercially available software (cvi42, Circle Cardiovascular Imaging). The superior and inferior vena cava were carefully excluded in slices in which they were clearly separated from the atrium or when there was no wall motion during atrial contraction (**Figure 2A**). Vena cava backflow was determined as described before.[5] In the larger cohort, RA volume was measured on the 4-chamber view using the area-length method. The right atrioventricular coupling index (RACI), a volumetric coupling ratio, was measured at: ventricular end-diastole (RA minimal volume / RV end-diastolic volume).[19]

RA PV LOOP ANALYSIS. A detailed description of the derivation of RA PV loops is given in the Supplemental Methods. The atrial phases of the PV loop (reservoir, passive emptying, and active emptying) were identified (**Figures 2B to 2D**). RA stroke work was measured as the area under the PV loop during atrial contraction. The pressure development during atrial contraction was called contractile pressure rise. Stiffness of the atrium and large veins was measured by fitting an exponential curve with the following equation: $P = \alpha(e^{\beta V} - 1)$ through 3 PV points (intercept [0,0], the x-descent and v-wave). The slope of this curve at the v-wave was called RA stiffness, analogous to RV end-diastolic elastance (E_{ed}), a measure of RV diastolic stiffness.[20] In the larger cohort in which RA volume was measured on the 4-chamber view, we estimated several PV loop parameters. RA stroke work was estimated through multiplying RA active emptying by a-wave pressure. Furthermore, RA stiffness was estimated with a linear formula: (v-wave pressure − x-descent pressure) / (v-wave volume − minimal volume). Both estimates of RA stroke work and RA stiffness correlated excellently with the original PV loop parameters (Supplemental Figure 1).

SINGLE CARDIOMYOCYTE AND HISTOLOGICAL ANALYSIS. Single RA cardiomyocytes were isolated and analyzed as described before for RV cardiomyocytes.[4,21] Details on the cardiomyocyte and histological analyses are provided in the Supplemental Methods.

STATISTICAL ANALYSIS. Statistical analyses were performed using R version 4.0.3 (R Foundation for Statistical Computing). Normality of data was checked prior to analysis. Non-normally distributed variables were normalized by logarithmic transformation (natural logarithm, base *e*) if possible. Data are presented as mean ± SD when normally distributed or median (IQR) plus reverse-transformed mean (95% CI) when non-normally distributed. Categorical variables are reported as number and percentage. Data in the figures are presented as mean ± SEM when normally distributed or reverse-transformed mean (95% CI) when non-normally distributed. Comparisons between groups were done with Fisher exact test, unpaired Student's *t*-test, or Wilcoxon's rank sum test. Comparison of multiple groups was done with analysis of variance and post hoc Tukey's test to correct for the familywise error rate. The homogeneity assumption was checked before testing by visually assessing the variance in all groups. Because the hypertrophy and capillary density analysis consisted of multiple observations per subject, we performed a multilevel analysis to assess differences between PAH patients and control subjects. All statistical tests were done with rstatix and visualization of data with ggplot2.

RESULTS

DISTINCT RA PV LOOP SHAPE IN precPH. We prospectively included idiopathic PAH (n = 13), hereditary PAH (n = 9), and CTEPH (n = 5) patients and healthy BMPR2 mutation carriers as control subjects (n = 9), who had a transverse RA stack of CMR images available, to construct PV loops (**Figure 1**). Characteristics and RA PV loop parameters in this cohort are shown in Supplemental Table 1. PV loops were averaged for the patient and control groups (**Figure 3**). The reservoir phase (atrial filling during ventricular contraction) is depicted in blue, passive emptying (early diastole) in red, and atrial contraction in purple. Three pressure points are labeled as the following: v-wave, end of ventricular contraction; a-wave, maximal pressure during atrial contraction; and x-descent, RA minimal pressure. Extensive RA dilatation was evident in precPH patients. RAP was higher in patients at the v-wave (9.5 mm Hg [IQR: 6.3-12.2 mm Hg] vs 6.5 mm Hg [IQR: 5.8-6.9 mm Hg]; $P = 0.002$) and a-wave (12.9 mm Hg [IQR: 10.0-16.2 mm Hg] vs 8.7 mm Hg [IQR: 8.1-9.3 mm Hg]; $P < 0.001$) but not at the x-descent (5.5 mm Hg [IQR: 1.8-6.6 mm Hg] vs 3.5 mm Hg [IQR: 2.1-4.2 mm Hg]; $P = 0.39$). Supplemental Figure 2 shows the mean pressure and the mean volume signal with a 95% CI. As there was only 1 patient with moderate tricuspid regurgitation (**Figure 2**) and no patients with severe regurgitation, this did not seem to impact the PV loop analysis. In all control subjects and patients, a-wave pressure was higher than v-wave pressure. RA active emptying and contractile pressure rise were higher in patients, resulting in a profound

FIGURE 4 Comparison of Patients With Moderate or Severe RV Diastolic Stiffness

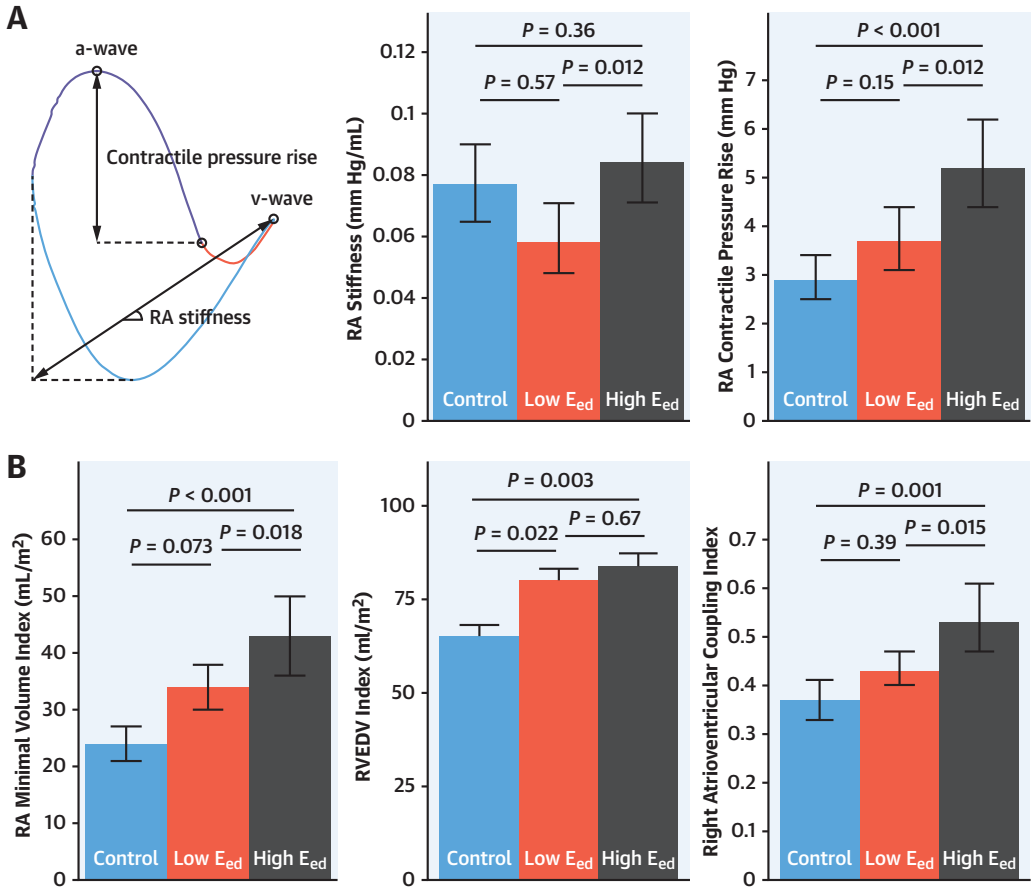

(A) RA stiffness was measured as the slope between the minimal pressure and volume point and v-wave. Contractile pressure rise is the pressure generated by atrial contraction. RA stiffness and contractile pressure rise were higher in severe right ventricular (RV) diastolic stiffness patients. **(B)** The right atrioventricular coupling index was calculated as follows: RA minimal volume / right ventricular end-diastolic volume (RVEDV). It was increased in patients with severe RV diastolic stiffness. Control group: n = 20; low end-diastolic elastance (E_{ed}) group: n = 39; high E_{ed} group: n = 41. Reverse log-transformed means and 95% CIs are presented, except for RVEDV for which the mean ± SEM is presented. Abbreviations as in Figures 1 and 2.

increase in RA stroke work (493 ± 253 mm Hg•mL vs 171 ± 50 mm Hg•mL; $P < 0.001$). We did not find differences in RA stiffness between patients and control subjects (0.33 mm Hg/mL [IQR: 0.24-0.64 mm Hg/mL] vs 0.26 mm Hg/mL [IQR: 0.23-0.37 mm Hg/mL]; $P = 0.22$).

ALTERED ATRIOVENTRICULAR COUPLING IN HIGH RV DIASTOLIC STIFFNESS PATIENTS. To better understand the relation between RV diastolic stiffness and atrioventricular coupling, we determined RA PV loop parameters in a larger cohort (Figure 1) of treatment-naive PAH patients (n = 80) and control subjects (n = 20). The PAH cohort predominantly consisted of female patients (68%), 57 ± 18 years of age, in NYHA functional class II/III. Similar to the PV loop cohort, mean RA, v-wave, and a-wave pressure were higher in precPH than in control subjects, while the x-descent pressure was not. Patients were equally distributed in either low RV E_{ed} (n = 39) or high RV E_{ed} (n = 41) according to a cutoff of 0.63 mm Hg/mL as previously described (Table 1).[5] Although RA stiffness was comparable in patients and control subjects (Figure 4A), high E_{ed} patients had slightly increased RA stiffness. A weak correlation between RA stiffness and RV E_{ed} was observed (Pearson $r = 0.28$; $P = 0.011$) (Supplemental Figure 3). Despite a larger pressure rise during RA contraction in high E_{ed} patients (Figure 4A), this did not result in enhanced RA active emptying (Table 1). To assess how well the RA was

FIGURE 5 Single Cardiomyocyte Measurements in Control Subjects and PrecPH Patients

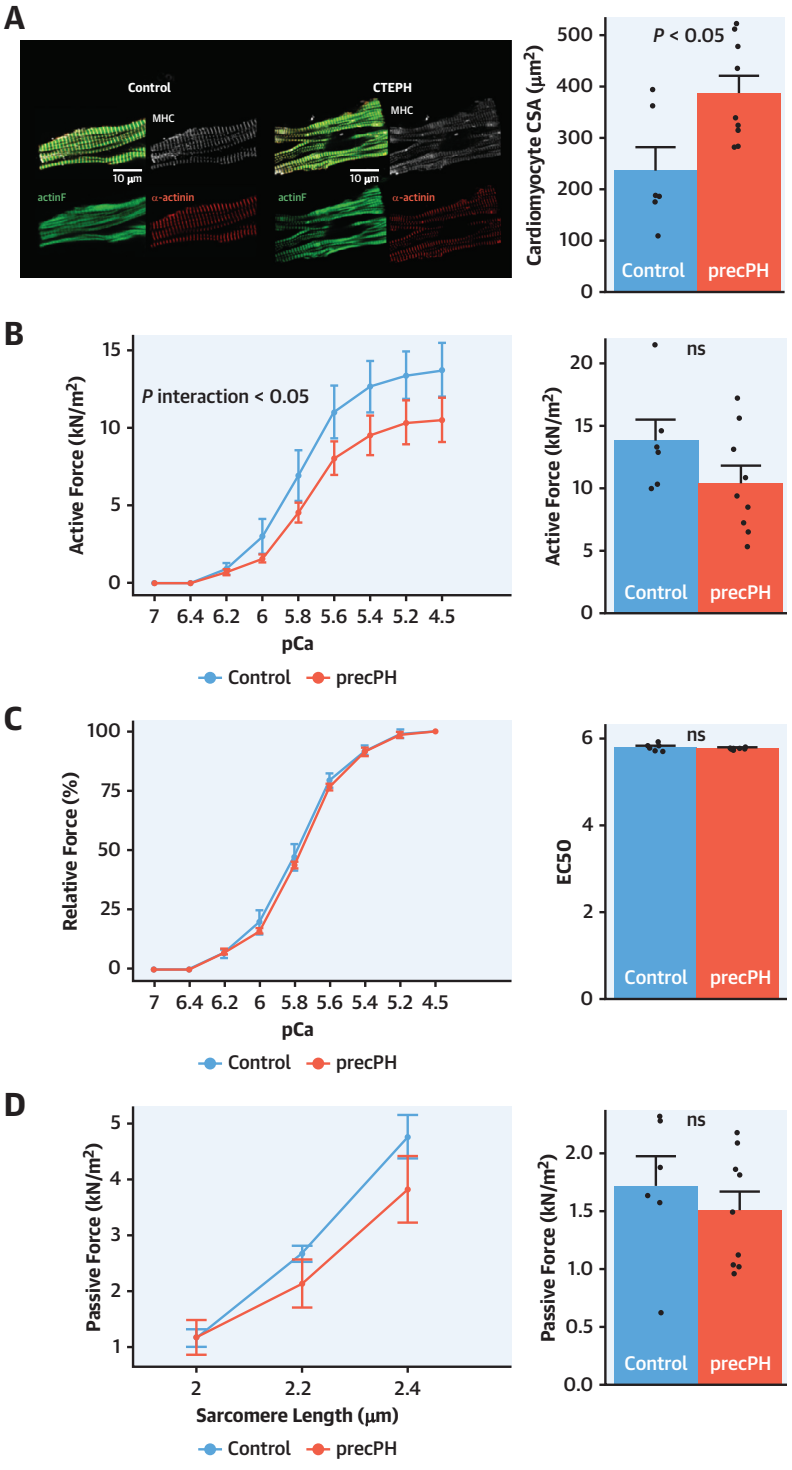

(A) Cardiomyocyte cross-sectional area (CSA) was increased in precapillary pulmonary hypertension (precPH) patients. **(B)** No difference in maximal active force generation was observed between control subjects and precPH patients. **(C)** The calcium concentration at which 50% of maximal force is generated (EC50) was not different between control subjects and precPH patients. **(D)** No difference in passive tension at increasing sarcomere length was found between control subjects and precPH patients. Control group: n = 6; precPH group: n = 9. pCa = inverse logarithmic calcium concentration.

adapted to the ventricle, we calculated the RACI, a volumetric coupling ratio measured at ventricular end-diastole (RA minimal volume / RV end-diastolic volume).[19] Although the RV end-diastolic volume was similar in low and high E_{ed} patients, in high E_{ed} patients this was accompanied by a larger RA minimal volume and therefore increased RACI (**Figure 4B**). This indicates that both the RA and ventricle are dilated but that the dilatation of the atrium is more severe in high E_{ed} patients. These data may further suggest that the adaptive capacity of the RA may be limited, resulting in altered atrioventricular coupling in patients with severe RV diastolic stiffness.

RA CARDIOMYOCYTE HYPERTROPHY IN precPH. Next, to study whether there are intrinsic changes in RA contractility and stiffness associated with pressure and volume overload, we isolated cardiomyocytes from 9 CTEPH and 6 age- and sex-matched control subjects (**Figure 1**, Supplemental Table 2). Hemodynamics and RV function of the CTEPH patients were comparable to the PAH cohort with mean pulmonary artery pressure of 49 ± 11 mm Hg, pulmonary vascular resistance of 8.6 ± 4.4 WU, and RV ejection fraction of 36% ± 16%. The RA cardiomyocyte cross-sectional area was significantly increased in precPH patients (**Figure 5A**). No difference was observed in maximal active force with or without correction of cross-sectional area (**Figure 5B**, Supplemental Figure 4). However, the force-generating capacity over the whole calcium concentration range was significantly different between the precPH and control groups (P interaction < 0.05) (**Figure 5B**). Relative force at different calcium concentrations was not different, indicating no difference in calcium sensitivity (**Figure 5C**). Last, passive force was similar in both groups at all sarcomere lengths, meaning that there was no difference in sarcomere stiffness, in line with the findings on RA stiffness in the PV loop analysis. These findings indicate that the sole adaptive feature of the RA at the cardiomyocyte level is hypertrophy. No intrinsic changes were seen in the sarcomeres themselves.

RA HYPERTROPHY AND FIBROSIS IN precPH. To confirm alterations in the RA at the histological level, we collected RA tissue postmortem or from transplanted PAH patients (**Figure 1**, Supplemental Table 3). We compared RA hypertrophy, capillary density, and fibrosis between end-stage disease patients and control subjects (**Figure 6**). In line with the increase in RA stroke work and single cardiomyocyte size, histology showed hypertrophy in precPH patients compared with control subjects. This was accompanied by an increase in the number of capillaries per cardiomyocyte (**Figures 6A to 6C**). When corrected for cardiomyocyte thickness, the number of capillaries per mm^2 was much lower in PAH (1,546 ± 384 vs 3,095 ± 889; $P < 0.01$). Both perivascular and interstitial fibrosis were significantly increased in RA tissue of PAH patients compared with control subjects (**Figures 6D to 6F**). These results show that in end-stage disease, the RA of PAH patients is affected by histological alterations including increased RA hypertrophy, a reduced number of capillaries per mm^2, and fibrosis.

DISCUSSION

Using PV loop, cardiomyocyte, and histopathological analysis, we provided an in-depth analysis of RA function in precPH (**Central Illustration**), which showed that: 1) RA stiffness, contractile pressure rise, and RACI were increased in patients with high RV E_{ed}, which may suggest altered atrioventricular coupling in patients with severe RV diastolic stiffness; 2) RA cardiomyocytes of precPH patients are hypertrophied but do not display intrinsic sarcomeric alterations including changes in active force, passive force, or calcium sensitivity; and 3) in end-stage disease, there is pronounced RA cardiomyocyte hypertrophy and both interstitial and perivascular fibrosis, and although the ratio of capillaries to cardiomyocytes is increased, the number of capillaries per mm^2 is reduced.

ATRIAL PV RELATION IN HEALTH AND DISEASE. Several studies have shown that RA pressure and volume are increased in precPH.[1,2,22,23] To study RA function in more detail, we constructed RA PV loops in both health and disease. Several animal studies have generated RA PV loops.[14-16] They have shown that contractility of the RA increases acutely after volume exposure, calcium or epinephrine infusion, and ischemia induction. Chronic increase in pressure overload and RV stiffening also results in increased RV contractility in animal models. Therefore, both an acute change in preload or sympathetic activity and chronically increased afterload lead to enhanced RA contraction to preserve RV filling. This is in line with our findings in precPH patients, who showed increased RA stroke work compared with control subjects. Interestingly, the RA PV loop shape in precPH patients is similar to RA PV loops generated in pressure overloaded dogs.[15] There is marked RA dilatation and increased pressure, mainly during the v-wave (ventricular contraction) and a-wave (atrial contraction). Passive emptying is diminished, while contractile pressure rise and active emptying are increased.

FIGURE 6 Histological Analysis of Hypertrophy, Capillarization, and Fibrosis

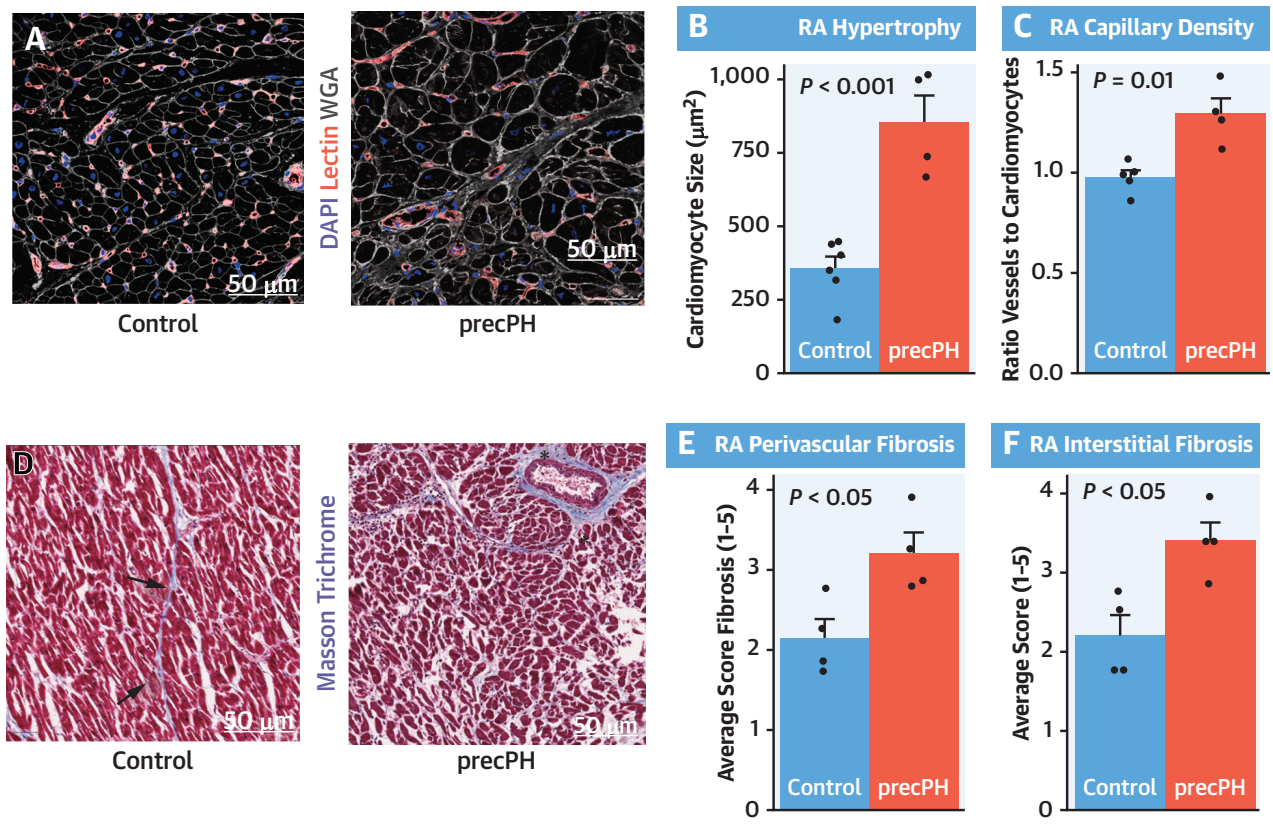

(A to C) Hypertrophy and capillarization was measured using DAPI, CD31, wheat germ agglutinin (WGA) staining. The cardiomyocyte size and number of vessels per cardiomyocyte were higher in precPH. **(D-F)** Fibrosis was assessed using Masson's trichrome staining. Perivascular **(asterisk)** and interstitial **(black arrows)** fibrosis were increased in precPH. Control group: n = 6; precPH group: n = 4. Abbreviations as in Figures 1 and 2.

DISTINCT RA PV LOOP PHENOTYPE. In contrast to previous descriptions of the left atrial (LA) PV loops, the RA PV loop does not have a closed v-loop and a-loop, but rather has a distinct shape.[10-13] There is only a small drop in pressure during early diastole. The pressure during passive emptying (orange phase in Figure 3) remains higher than during the reservoir phase. The larger drop in pressure in the LA may be a consequence of left ventricular early diastolic suction.[24] In healthy control subjects, LA v-wave and a-wave pressure show similarities to our findings in the RA.[11-13] a-wave pressure is higher than v-wave pressure and a-loop area larger than v-loop area. In diseased patients, however, differences between RA and LA PV loops become more evident. We observed higher RA a-wave than v-wave pressure in all precPH patients, also when a moderate-to-severe tricuspid regurgitation is present (Figure 2). This is in line with a previous report on atrial septal defect, providing 2 example RA PV loops.[25] In contrast, in congestive heart failure, a relatively larger increase in LA v-wave pressure compared with a-wave pressure is observed.[11,12] Furthermore, LA stiffness was significantly increased in congestive heart failure, heart failure with preserved ejection fraction, and persistent atrial fibrillation patients.[26,27] In our study, we did not find a difference in RA stiffness or cardiomyocyte stiffness between precPH patients and control subjects.[28] Therefore, the response of the RA to pressure and/or volume overload may be different from the LA.

ATRIOVENTRICULAR INTERACTION AND ALTERED COUPLING IN PATIENTS WITH SEVERE RV DIASTOLIC STIFFNESS. Reduced forward flow and RV diastolic stiffening lead to increased filling pressures and afterload for the RA. Tricuspid regurgitation leads to a volume overload on both the ventricle and atrium. In addition, a large amount of backflow to the vena cava induces a further volume overload on the atrium.[5,6] This volume overload is probably the main cause of RA dilatation. To better understand whether changes in RA parameters reflect the failing and stiff RV or

CENTRAL ILLUSTRATION **Right Atrial Adaptation in Pulmonary Hypertension**

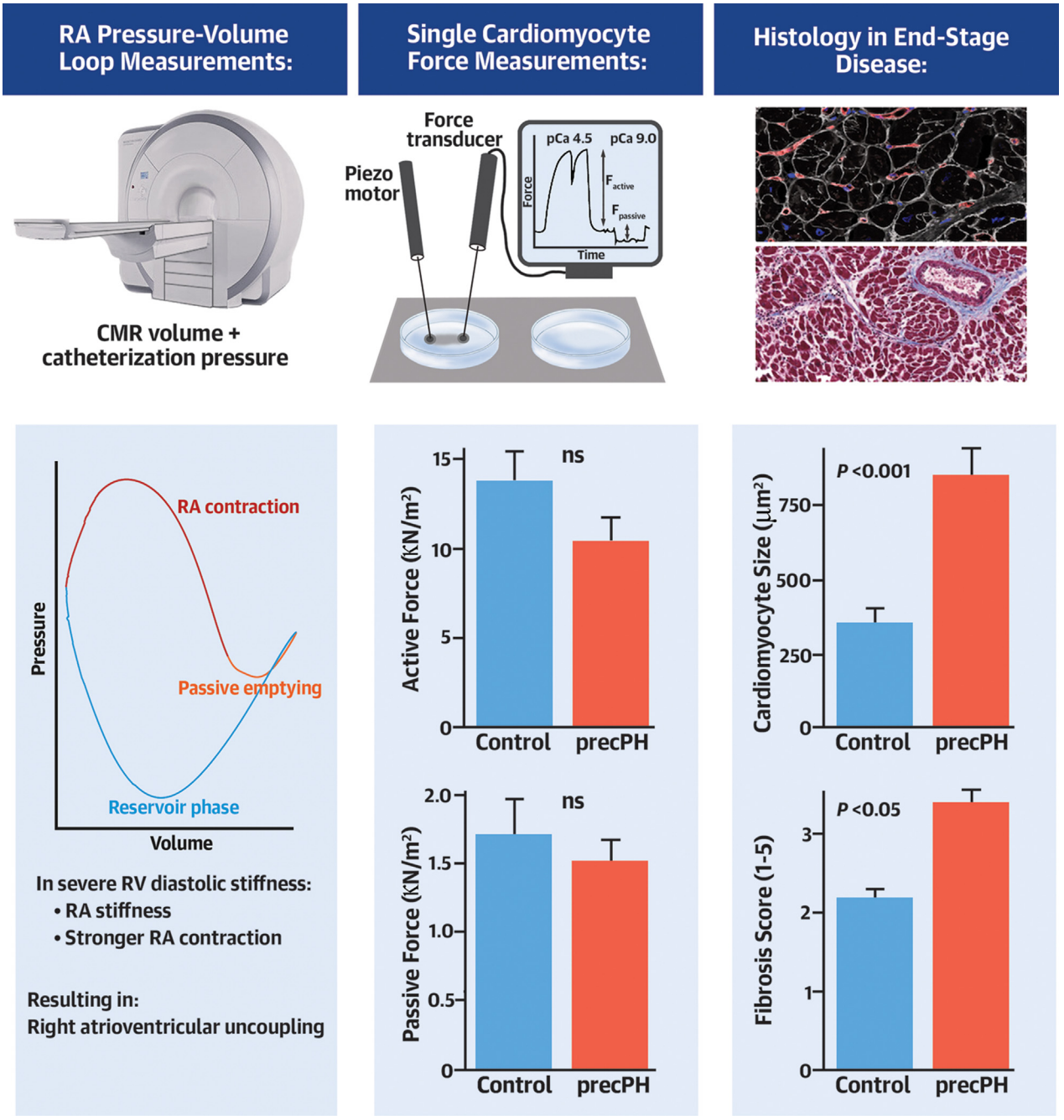

Wessels JN, et al. J Am Coll Cardiol. 2023;82(8):704–717.

This figure summarizes findings of the study. Right atrial (RA) pressure-volume loops were constructed using cardiac magnetic resonance (CMR) volume and pressure data and showed 3 distinct RA phases. Single cardiomyocyte force measurements showed no differences in sarcomere function between precapillary pulmonary hypertension (precPH) and control subjects. Histology showed hypertrophy and both interstitial and perivascular fibrosis in precPH. RV = right ventricular.

whether these are independent contributors to the clinical right heart failure syndrome, we assessed the interaction between the RA and RV. Signs of RA adaptation include hypertrophy and increased stroke work. The resulting increase in RA active emptying may preserve RV filling in low E_{ed} patients but is not sufficient in high E_{ed} patients.[5] Furthermore, the RACI is worse in high vs low E_{ed} patients. There is relatively more dilatation of the atrium than of the ventricle. This can be explained by the larger volume overload on the atrium because of vena cava backflow in high E_{ed} patients. Tricuspid regurgitation may add to the volume overload but is similar in low and high E_{ed} patients.[5] Although these findings may suggest altered atrioventricular coupling, it remains unclear whether a further augmentation of RA stroke work would lead to better RV filling or whether it would result in more vena cava backflow.

RA HYPERTROPHY AND CONTRACTILITY IN precPH. We previously reported a large increase in RA stroke work in precPH patients, also shown by the RA PV loop in this study.[5] Augmented stroke work can be the result of increased cardiomyocyte contractility and/or hypertrophy. Indeed, both single RA cardiomyocyte and histological analysis showed an up to 3-fold increase in cross-sectional area compared with control subjects. Interestingly, maximal force was not higher in precPH. Force-generating capacity across the range of calcium concentrations was even slightly diminished. This is in line with previous RA cardiomyocyte measurements of patients with atrial fibrillation.[28] It could be hypothesized that the hypertrophy may compensate for the subtle loss of force-generating capacity at the cellular level. However, future longitudinal analyses of RA adaptation and diastolic stiffness should reveal whether RA cardiomyocytes are unable to intrinsically increase contractility or whether hypertrophy obviates the need for increased sarcomere contractility.

RA CAPILLARIZATION AND FIBROSIS IN precPH. The observation of substantial hypertrophy of RA cardiomyocytes raises the question of whether capillarization is also augmented. Although the number of vessels per cardiomyocyte was increased in end-stage disease patients, the number of vessels per mm^2 was decreased to about one-half the value in control subjects. Reduction to a similar degree was observed in the RV, in which hypertrophy of RV cardiomyocytes was associated with reduced capillary density.[29] In addition, both interstitial and perivascular RA fibrosis were observed. This may suggest that in end-stage disease RA compensation is insufficient and increased RA stiffness is expected in end-stage disease. Unfortunately, no RA functional data were available at end-stage disease to assess the functional relevance of this increase in RA fibrosis. Future longitudinal analyses should reveal the timing of RA hypertrophy, capillary rarefaction, fibrosis, and RA stiffness.[4,30]

CLINICAL RELEVANCE. Because RA pressure and volume are associated with mortality, they are incorporated in the risk stratification model in PAH.[3] A mean RAP of 8 to 14 mm Hg is associated with intermediate risk and a mean RAP >14 mm Hg is associated with high risk of 1-year mortality. Our PV loop analysis shows that RA pressure in precPH is mainly elevated at the v-wave and a-wave. These pressure points can be identified automatically during catheterization and may entail better prognostic value than mean RAP. For RA area, the guideline also provides mortality risk cutoffs at baseline and in a recent study, RA dilatation had predictive value at first follow-up in addition to functional class, 6-minute walking distance, and N-terminal pro-B-type natriuretic peptide levels.[23] The current data show that RA dilatation is relatively greater than RV dilatation in patients with severe RV diastolic stiffness. It should be further investigated whether assessment of RA-RV coupling may provide additional prognostic information than RA area alone.

Atrioventricular uncoupling in patients with severe RV diastolic stiffness results in vena cava backflow and congestion, which may be worsened by tricuspid regurgitation. This can have serious consequences such as hepatic fibrosis and cirrhosis, congestive nephropathy, ascites, leaky bowel syndrome, and peripheral edema. There is therefore an unmet need for the development of medication targeting RV diastolic stiffening to restore RA-RV interaction.

STUDY LIMITATIONS. This was a single-center study that consisted of 4 different cohorts, both prospective and retrospective. One-half of the patients in the RA PV loop cohort received treatment, whereas all patients in the 4-chamber cohort were treatment naive. Cardiomyocytes were isolated from CTEPH patients and not from PAH patients. Cardiomyocyte analyses are best performed in freshly collected tissue samples which could only be obtained from CTEPH patients undergoing pulmonary endarterectomy. Nevertheless, we expect that potential bias of differences in the patient cohort is negligible, as the patient characteristics were similar, and a previous comparison between cardiac adaptation of CTEPH and PAH patients showed no large differences.[30] Finally, the RA tissue sample size (used for cardiomyocyte and histopathological analyses) was small due to the limited access to fresh tissue. Nevertheless, we observed clear

differences in RA hypertrophy, capillarization, and fibrosis. The histopathological analysis was performed on autopsy material because the RA tissue samples that were collected during pulmonary endarterectomy were too small for both cardiomyocyte and histopathological analysis. Therefore, it is unclear whether fibrosis is already present in incident precPH patients.

CONCLUSIONS

RA PV loops show increased RA stiffness and suggest atrioventricular uncoupling in patients with severe RV diastolic stiffness. Isolated RA cardiomyocytes of precPH patients are hypertrophied but do not display intrinsic sarcomeric changes in active or passive force. In end-stage pulmonary hypertension, reduced capillary density as well as interstitial and perivascular fibrosis are observed.

ACKNOWLEDGMENT The authors thank prof.dr. Coen Ottenheijm and Stefan Conijn of the Department of Physiology, Amsterdam UMC for their introduction and support on the cardiomyocyte set-up.

FUNDING SUPPORT AND AUTHOR DISCLOSURES

Drs Bogaard, Vonk Noordegraaf, Goumans, and de Man were supported by the Netherlands CardioVascular Research Initiative: the Dutch Heart Foundation, Dutch Federation of University Medical Centres, the Netherlands Organisation for Health Research and Development, and the Royal Netherlands Academy of Sciences (CVON-2012-08 PHAEDRA, CVON-2018-29 PHAEDRA-IMPACT, and CVON-2017-10 Dolphin-Genesis). Drs Vonk Noordegraaf and de Man were further supported by the Netherlands Organization for Scientific Research (NWO-VICI: 918.16.610, NWO-VIDI: 917.18.338). Dr de Man was supported by a Dutch Heart Foundation Dekker senior postdoc grant (2018T059). Drs Bogaard and Vonk Noordegraaf have received research grant support from Actelion, GSK, and Ferrer (Therabel). Dr de Man has received research grant support from Janssen and BIAL. Dr Handoko has received consultancy/speaker fees from Novartis, Boehringer Ingelheim, AstraZeneca, Vifor, Bayer, MSD, and Abbott. All other authors have reported that they have no relationships relevant to the contents of this paper to disclose.

ADDRESS FOR CORRESPONDENCE: Dr Frances de Man, Amsterdam UMC location Vrije Universiteit Amsterdam, PHEniX Laboratory, Department of Pulmonary Medicine, Amsterdam Cardiovascular Sciences, Pulmonary Hypertension and Thrombosis, De Boelelaan 1117, 1081 HV Amsterdam, the Netherlands. E-mail: fs.deman@amsterdamumc.nl.

PERSPECTIVES

COMPETENCY IN MEDICAL KNOWLEDGE: Severe RV diastolic stiffness is associated with atrioventricular uncoupling, RA stiffness, hypertrophy, fibrosis, and reduced capillary density without atrial sarcomere dysfunction.

TRANSLATIONAL OUTLOOK: Because RA dysfunction is a consequence of RV stiffening rather than of atrial sarcomeric dysfunction in patients with precPH, treatment strategies should focus on improving RV diastolic function.

REFERENCES

1. Nickel N, Golpon H, Greer M, et al. The prognostic impact of follow-up assessments in patients with idiopathic pulmonary arterial hypertension. *Eur Respir J*. 2012;39:589–596.

2. Raymond RJ, Hinderliter AL, Willis PW, et al. Echocardiographic predictors of adverse outcomes in primary pulmonary hypertension. *J Am Coll Cardiol*. 2002;39:1214–1219.

3. Humbert M, Kovacs G, Hoeper MM, et al. 2022 ESC/ERS Guidelines for the diagnosis and treatment of pulmonary hypertension. *Eur Respir J*. 2023;61:2200879.

4. Rain S, Handoko ML, Trip P, et al. Right ventricular diastolic impairment in patients with pulmonary arterial hypertension. *Circulation*. 2013;128:2016–2025.

5. Wessels JN, Mouratoglou SA, van Wezenbeek J, et al. Right atrial function is associated with RV diastolic stiffness: RA-RV interaction in pulmonary arterial hypertension. *Eur Respi J*. 2022;59:2101454.

6. Marcus JT, Westerhof BE, Groeneveldt JA, Bogaard HJ, de Man FS, Noordegraaf AV. Vena cava backflow and right ventricular stiffness in pulmonary arterial hypertension. *Eur Respir J*. 2019;54:1900625.

7. Tello K, Dalmer A, Vanderpool R, et al. Right ventricular function correlates of right atrial strain in pulmonary hypertension: a combined cardiac magnetic resonance and conductance catheter study. *Am J Physiol Heart Circ Physiol*. 2020;318:H156–H164.

8. Alenezi F, Mandawat A, Il'Giovine ZJ, et al. Clinical utility and prognostic value of right atrial function in pulmonary hypertension. *Circ Cardiovasc Imaging*. 2018;11:e006984.

9. Leng S, Dong Y, Wu Y, et al. Impaired cardiovascular magnetic resonance-derived rapid semi-automated right atrial longitudinal strain is associated with decompensated hemodynamics in pulmonary arterial hypertension. *Circ Cardiovasc Imaging*. 2019;12:e008582.

10. Alexander J Jr, Sunagawa K, Chang N, Sagawa K, Building T. Instantaneous pressure-volume relation of the ejecting canine left atrium. *Circ Res*. 1987;61:209–219.

11. Dernellis JM, Stefanadis CI, Zacharoulis AA, Toutouzas PK. Left atrial mechanical adaptation to long-standing hemodynamic loads based on pressure-volume relations. *Am J Cardiol*. 1998;81:1138–1143.

12. Stefanadis C, Dernellis J. Assessment of left atrial pressure-area relation in humans by means of retrograde left atrial catheterization and echocardiographic automatic boundary detection: effects of dobutamine. *J Am Coll Cardiol*. 1998;31:426–436.

13. Stefanadis C, Dernellis J, Stratos C, et al. Effects of balloon mitral valvuloplasty on left atrial function in mitral stenosis as assessed by pressure-area relation. *J Am Coll Cardiol*. 1998;32:159–168.

14. Lau V-K, Sagawa K, Suga H. Instantaneous pressure-volume relationship of right atrium during isovolumic contraction in canine heart. *Am J Physiol*. 1979;236:H672–H679.

15. Gaynor SL, Maniar HS, Bloch JB, Steendijk P, Moon MR. Right atrial and ventricular adaptation

to chronic right ventricular pressure overload. *Circulation*. 2005;112:212–218.

16. Goldstein JA, Tweddell JS, Barzilai B, et al. Right atrial ischemia exacerbates hemodynamic compromise associated with experimental right ventricular dysfunction. *J Am Coll Cardiol*. 1991;18:1564–1572.

17. van Wezenbeek J, Groeneveldt JA, Llucià-Valldeperas A, et al. Interplay of sex hormones and long-term right ventricular adaptation in a Dutch PAH-cohort. *J Heart Lung Transplant*. 2022;41:445–457.

18. van de Veerdonk MC, Kind T, Marcus JT, et al. Progressive right ventricular dysfunction in patients with pulmonary arterial hypertension responding to therapy. *J Am Coll Cardiol*. 2011;58:2511–2519.

19. Pezel T, Venkatesh BA, de Vasconcellos HD, et al. Left atrioventricular coupling index as a prognostic marker of cardiovascular events: the MESA study. *Hypertension*. 2021;78:661–671.

20. Trip P, Rain S, Handoko ML, et al. Clinical relevance of right ventricular diastolic stiffness in pulmonary hypertension. *Eur Respir J*. 2015;45:1603–1612.

21. van der Velden J, Klein LJ, van der Bijl M, et al. Isometric tension development and its calcium sensitivity in skinned myocyte-sized preparations from different regions of the human heart. *Cardiovasc Res*. 1999;42:706–719.

22. Querejeta Roca G, Campbell P, Claggett B, Solomon SD, Shah AM. Right atrial function in pulmonary arterial hypertension. *Circ Cardiovasc Imaging*. 2015;8:e003521.

23. Shah T, Manthena P, Patel C, et al. Prognostic value of echocardiographic variables prior to and following initiation of parenteral prostacyclin therapy: an observational study. *Chest*. 2022;162:669–683.

24. Nakatani S, Beppu S, Nagata S, et al. Diastolic suction in the human ventricle: observation during balloon mitral valvuloplasty with a single balloon. *Am Heart J*. 1994;127:143–150.

25. Ferguson JJ, Miller MJ, Aroesty JM, Sahagian P, Grossman W, Mckay RG. Assessment of right atrial pressure-volume relations in patients with and without an atrial septal defect. *J Am Coll Cardiol*. 1989;13:630–636.

26. Melenovsky V, Hwang SJ, Redfield MM, Zakeri R, Lin G, Borlaug BA. Left atrial remodeling and function in advanced heart failure with preserved or reduced ejection fraction. *Circ Heart Fail*. 2015;8:295–303.

27. Khurram IM, Maqbool F, Berger RD, et al. Association between left atrial stiffness index and atrial fibrillation recurrence in patients undergoing left atrial ablation. *Circ Arrhythm Electrophysiol*. 2016;9:e003163.

28. Eiras S, Narolska NA, van Loon RB, et al. Alterations in contractile protein composition and function in human atrial dilatation and atrial fibrillation. *J Mol Cell Cardiol*. 2006;41:467–477.

29. Ruiter G, Ying Wong Y, de Man FS, et al. Right ventricular oxygen supply parameters are decreased in human and experimental pulmonary hypertension. *J Heart Lung Transplan*. 2013;32:231–240.

30. Braams NJ, van Leeuwen JW, Vonk Noordegraaf A, et al. Right ventricular adaptation to pressure-overload: differences between chronic thromboembolic pulmonary hypertension and idiopathic pulmonary arterial hypertension. *J Heart Lung Transplant*. 2021;40:458–466.

KEY WORDS pressure-volume loop, pulmonary arterial hypertension, right atrioventricular coupling, right atrium, right ventricle

APPENDIX For expanded Methods and References sections as well as supplemental figures and tables, please see the online version of this paper.